

Generation of ultra-flat broad spectrum with stable single-pulse mode-locking in double-clad Yb-doped fiber laser

Minghui Sun(孙铭烩), Dongxin Gao(高懂昕), Yunli Yu(于芸丽), Wenyu Wang(王文煜), Qingcao Liu(刘情操), Weixin Liu(刘维新), and Yuzhai Pan(潘玉寨)

Citation: Chin. Phys. B, 2026, 35 (**1**): 014206. DOI: 10.1088/1674-1056/adea59
http://cpb.iphy.ac.cn; http://iopscience.iop.org/cpb

What follows is a list of articles you may be interested in

Synchronized dual-wavelength mode-locked laser in normal dispersion regime

Yangrui Shi(史洋瑞), Haojing Zhang(张皓景), Yuxuan Ren(任俞宣), Junsong Peng(彭俊松), and Heping Zeng(曾和平)

Chin. Phys. B, 2025, 34 (**9**): 094207. DOI: 10.1088/1674-1056/add4fe

Generation ofWatt-level Kerr-lens mode-locked Yb:CYA laser at 1-GHz repetition rate

Guodong Zhao(赵国栋), Junyi Ma(马骏逸), Hainian Han(韩海年), Zhaohua Wang(王兆华), and Zhiyi Wei(魏志义)

Chin. Phys. B, 2025, 34 (**8**): 084204. DOI: 10.1088/1674-1056/adcf8b

High stability and low noise laser-diode end-pumped Nd: YAG ceramic passively *Q*-switched laser at 1123 nm based on a $Ti_3C_2T_x$-PVA saturable absorber

Jia-Le Yan(闫佳乐), Ben Li(李奔), Guo-Zhen Wang(王国珍), Shun-Yu Yang(杨顺宇), Bao-Le Lu(陆宝乐), and Yang Bai(白杨)

Chin. Phys. B, 2023, 32 (**11**): 114212. DOI: 10.1088/1674-1056/acf495

Simultaneous detection of CH_4 and CO_2 through dual modulation off-axis integrated cavity output spectroscopy

Yi-Xuan Liu(刘艺璇), Zhou-Bing Wang(王周兵), Xin-Xin Wei(韦欣欣), Jing-Jing Wang(王静静), Xin Meng(孟鑫), and Gui-Lin Mao(毛桂林)

Chin. Phys. B, 2023, 32 (**10**): 104209. DOI: 10.1088/1674-1056/acdac1

High sensitivity plasmonic temperature sensor based on a side-polished photonic crystal fiber

Zhigang Gao(高治刚), Xili Jing(井西利), Yundong Liu(刘云东), Hailiang Chen(陈海良), and Shuguang Li(李曙光)

Chin. Phys. B, 2022, 31 (**2**): 024207. DOI: 10.1088/1674-1056/ac0a63

Generation of ultra-flat broad spectrum with stable single-pulse mode-locking in double-clad Yb-doped fiber laser

Minghui Sun(孙铭烩)[1], Dongxin Gao(高懂昕)[1], Yunli Yu(于芸丽)[1], Wenyu Wang(王文煜)[1], Qingcao Liu(刘情操)[1], Weixin Liu(刘维新)[2], and Yuzhai Pan(潘玉寨)[1,†]

[1] *Department of Optoelectronics Science, Harbin Institute of Technology (Weihai), Weihai* 264209, *China*
[2] *Shandong Provincial Key Laboratory of Optical Astronomy and Solar-Terrestrial Environment, Institute of Space Sciences, Shandong University, Weihai* 264209, *China*

(Received 18 April 2025; revised manuscript received 13 June 2025; accepted manuscript online 1 July 2025)

We achieved an ultra-flat broad spectrum output with a 20-dB bandwidth of 77.85 nm in a double-clad Yb-doped fiber laser. The intensity difference between the highest and lowest points of the spectrum indicates a flatness better than 4 dB. More notably, this ultra-flat broad spectrum maintains a stable single-pulse mode-locking state. With the increase of pump power, an ultra-wide spectrum with a 20-dB bandwidth approaching 100 nm was formed at a pump power of 2.25 W. Additionally, we obtained a 9-pulse mode-locked state at another PC station with the same pump, which is the highest number of stable mode-locked pulse bursts observed so far with a first-order Raman frequency shift. This fiber laser shows its benefits of ultra-flat broad spectrum, high stability, and ease of fabrication, which provides a new method of obtaining the broadband light source for multiple practical applications.

Keywords: ultra-flat broad spectrum, high stability, double-clad Yb-doped fiber, mode-locked, multi-pulse bursts

PACS: 42.55.Wd, 42.60.Fc

DOI: 10.1088/1674-1056/adea59 **CSTR:** 32038.14.CPB.adea59

1. Introduction

Passive mode-locked fiber lasers are widely used in nonlinear optics,[1,2] optical clock,[3] micromachining,[4] and supercontinuum (SC) generation[5–7] due to their advantages such as compact structure, low cost and long-term stability.[8,9] It has been reported that there are many effective methods to achieve passive mode-locking in lasers, including semiconductor saturable absorption mirrors (SESAMs),[10] nonlinear polarization rotation (NPR)[11–14] and two-dimensional (2D) nanomaterials.[15–17] Among them, the NPR mechanism has the advantages of significant modulation depth, design flexibility, and ultra-short response time,[12,14] making it a common technology to achieve mode-locked pulses in fiber lasers. NPR mode-locked lasers can produce wide spectral widths[18] without needing external fiber components, such as dedicated nonlinear fibers or double-clad power amplifiers. This no-additional-requirements feature simplifies operational setup and makes SC sources a more robust, economically viable, and easy-to-operate single-system solution.[19]

Broadband sources, due to their unique combination of coherence, brightness, and spectral breadth, have enabled critical applications from biomedical imaging to industrial sensing.[20–23] Wider SCs can extend the spectrum into the mid-infrared region and play an important role in defense and healthcare.[24] Recently, fiber lasers operating in a pulsed state have been used for SC generation.[25,26] SC generation is a phenomenon that occurs due to the combination and interaction of nonlinear optical effects and scattering, and is notably characterized by extreme spectral broadening.[27,28] The nonlinear optical effects that lead to the formation of SC include self-phase modulation (SPM), intermodal interference (MI), stimulated Raman scattering (SRS), and four-wave mixing (FWM), and the scattering effects include group velocity dispersion (GVD).[27,29]

Supercontinuum generation (SCG) in fiber lasers is achieved through two principal approaches: external pumping of nonlinear fibers and intracavity SCG technology. While the former requires complex systems with substantial cost overhead, the latter enables direct spectral broadening within the laser cavity via an all-fiber architecture, offering superior compactness and reduced component count.[19,30] In 2020, Carrillo-Delgado *et al.* designed a Yb-doped fiber laser(YDFL),[31] which achieved an intracavity broadband spectrum of 1020 nm–1160 nm. However, the output broadband spectrum of the laser showed a limited temporal performance. In 2022, Bin Zhang *et al.* developed a Yb-doped intracavity cascade Raman fiber laser based on NPR,[32] and obtained a broadband spectrum with a 3-dB bandwidth of 48.50 nm at a pump power of 945 mW. The broadband spectral

[†]Corresponding author. E-mail: panyz@hitwh.edu.cn

© 2026 Chinese Physical Society and IOP Publishing Ltd. All rights, including for text and data mining, AI training, and similar technologies, are reserved.

state remains single-pulse mode-locking, but this single pulse had an irregular shape with non-negligible temporal fluctuations at the front of the pulse. In 2023, Cruz *et al*. built a 9-character YDFL,[30] which realized intra-cavity SCG. The SC extending from visible light to more than 2 μm was obtained at a pump power of 3 W. However, due to the cavity design of the semi-open configuration of the 9-figure laser cavity, the pulse exhibited significant intensity jitter and presented compromised temporal stability. In the same year, Manriquez-Cobian *et al*. designed an NPR-based ring cavity YDFL to achieve SRS by increasing the pump power,[33] obtaining the formation of up to four Stokes waves, thus achieving a spectral broadening of 200 nm. However, the time domain measurement results of pulses are still not ideal, and their separation is not uniform in addition to the complex shape of pulses. In 2024, Ahmad *et al*. designed a YDFL based on the NPR.[19] The YDFL can generate noise-like pulse (NLP), and increasing the pump power from the NLP state can produce a flat 5-dB SC wider than 320 nm. However, the study does not give the pulse state when the laser outputs an SC.

In summary, achieving simultaneous wide bandwidth, highly flat ultra-wide spectrum and stable single-pulse mode-locked remains a critical challenge in current research, which essentially requires precise control of intracavity nonlinear dynamics through sophisticated cavity design. The key lies in establishing optimal cavity conditions including dispersion management, nonlinear regulation, and gain optimization. While previous studies have demonstrated various spectral broadening mechanisms,[31,33–35] our work focuses on maintaining robust single-pulse operation throughout the SCG process.

This paper provides a new method of obtaining the broadband light source based on the NPR mechanism. A wide spectrum with a flatness better than 4 dB was obtained, which has a 20-dB bandwidth of 77.85 nm. With a further increase in pump power, the spectrum continued to widen to nearly 100 nm. Furthermore, the generation of adjustable pulse bursts is realized with the change of pump power. A pulse burst with a pulse number of 9 was obtained at a pump power of 2.25 W. As far as we know, this is the 9-pulse mode-locked with the largest number of pulses in the current pulse bursts phenomenon with first-order Raman frequency shift.[33,34,36]

2. Experimental setup

Figure 1 illustrates the experimental setup of the double-clad Yb-doped fiber laser based on the NPR technique. The gain medium is a 20-m double-clad Yb-doped fiber (Liekki, Yb1200-6/125DC) with group velocity dispersion (GVD) of ~ 24 ps^2/km at 1060 nm, pumped by a multi-mode pump laser diode (LD) with a maximum pump power of 9 W through a pump combiner. A polarization-dependent isolator (PD-ISO) and two polarization controllers (PCs) are used as the key NPR mode-locking components, ensuring the unidirectional transmission of optical pulses within the cavity for mode-locking operation. The PCs adjust the optical polarization in the cavity by rotating a polarizer to optimize the mode-locking state. A $\sim$ 235-m single-mode fiber (SMF) (Corning, HI1060) with GVD of ~ 23 ps^2/km at 1060 nm is used as the Raman gain medium within the cavity. The total cavity length is approximately 265 m, with all fibers and device pigtails in the experimental system being HI1060 fiber, except for the gain fiber. The net dispersion of the laser cavity is estimated about ~ 6.12 ps^2. The laser performance is monitored at the 20% output port using an 80:20 optical coupler (OC).

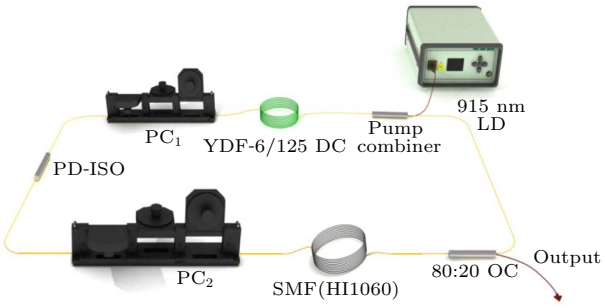


Fig. 1. Experimental setup of NPR mode-locked double-clad Yb-doped fiber laser

The output laser is divided by a 10/90 beam splitter, with the spectrum and pulse information observed by an optical spectrum analyzer (Anritsu, MS9710C with a resolution of 0.05 nm) and a digital oscilloscope (GWINSTEK, GDS-2202A, bandwidth 200 MHz, real-time sampling rate 2 GSa/s), respectively. The operational stability of the cavity is investigated using a radio frequency (RF) spectrum analyzer (9 kHz–3.25 GHz, GSP-9330), and the average output power is measured with an optical power meter (FieldBest) with a maximum range of 6 W.

3. Results and discussion

3.1. Generation of the flat broadband spectrum with stable single pulse

As the pump power increased to 0.38 W and the PC state was properly adjusted, the self-starting passively mode-locked pulses were generated, and a typical first-order SRS was obtained. Figure 2 shows the output characteristics of the passively mode-locked fiber laser at a pump power of 0.38 W. Figure 2(a) displays a spectrum centered at 1109.2 nm with a 20-dB spectral bandwidth of 73.45 nm. The center wavelengths of the fundamental light and first-order Stokes light are 1078.3 nm and 1135.5 nm, respectively, with a wavelength difference of 57.2 nm and a corresponding frequency shift of approximately 14 THz. This aligns with the typical Raman

shift of 13 THz–15 THz in standard single-mode fibers, attributing the spectrum peak at 1135.5 nm to intracavity Raman conversion.

The pulse sequence and corresponding single pulse at this state are shown in Figs. 2(b) and 2(c). The time interval of the pulse sequence is 1.32 μs, consistent with the cavity's round-trip time. The full width at the half of maximum (FWHM) of the pulse is 3.85 ns, and the wide width of the pulse is mainly due to the large net dispersion introduced by the long laser cavity length. Since Raman light moves faster than fundamental frequency light in the normal group velocity dispersion (GVD) regime, the pulse combination of the fundamental frequency laser and the Raman laser results in an asymmetric pulse shape with steeper leading,[37] as depicted in Fig. 2(c). Figure 2(d) shows the RF spectrum of the pulse with a fundamental frequency repetition of 755 kHz and signal-to-noise ratio (SNR) of ∼ 59 dB, implying a stable mode-locked operation. The inset of Fig. 2(d) depicts the RF spectrum spanning 50 MHz with no periodic envelope or fluctuation, meaning that the laser operates well in a stable single-pulse mode-locking state. The average output power is 2 mW, corresponding to a single pulse energy of 2.65 nJ, under the pump power of 380 mW in the single-pulse mode.

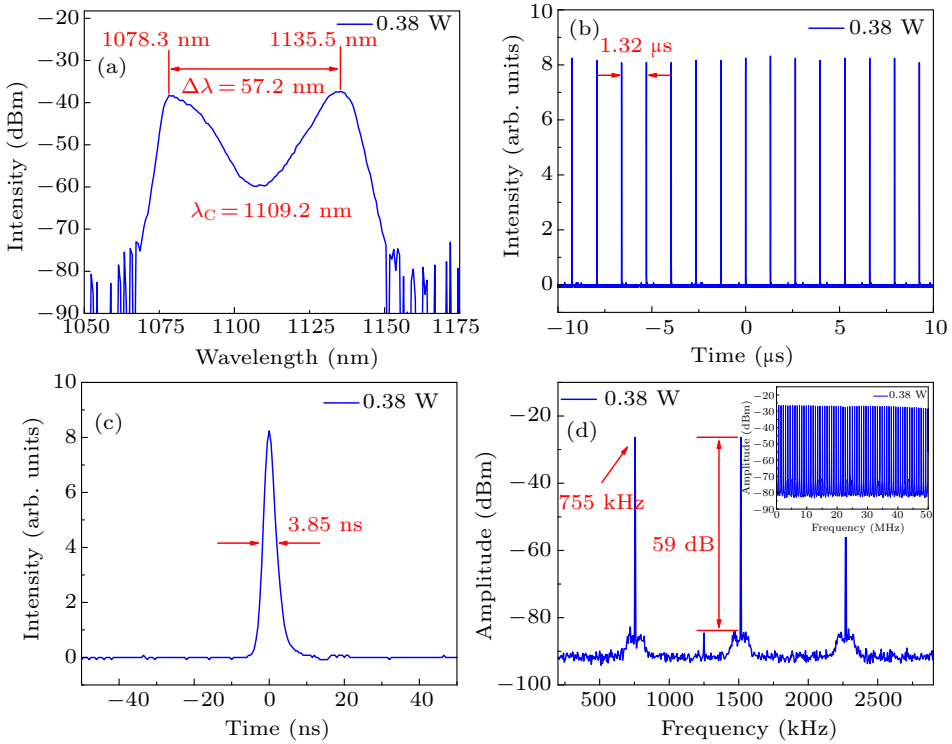


Fig. 2. Output characteristics of the laser at a pump power of 0.38 W: (a) spectrum, (b) pulse sequence, (c) single pulse, (d) RF spectrum with a fundamental frequency of 755 kHz (inset: RF spectrum with a bandwidth of 0 MHz–50 MHz).

After the above experiments, by slightly adjusting two PCs at a pump power of 0.5 W, we achieved an ultra-flat broad spectrum output with a 20-dB bandwidth of 77.85 nm and a 6-dB bandwidth of 67.5 nm, as shown in Fig. 3(a). The intensity difference between the highest point (−38.42 dBm) and the lowest point (−41.80 dBm) of the spectrum is only 3.38 dB, indicating a flatness better than 4 dB, which combines both width and flatness.

The pulse sequence and corresponding single pulse with the ultra-flat wide spectrum state are shown in Figs. 3(b) and 3(c). The time interval of the pulse sequence is 1.32 μs, which is consistent with the cavity round-trip time. The full width at the half of maximum (FWHM) of the pulse is 5.15 ns. Unlike previous studies where pulse outputs in broad spectrum states were chaotic and irregular,[30,31,33] our fiber laser design ensures a stable single-pulse mode-locking state while outputting a super-flat broad spectrum. In order to prove that our laser can output a smooth and wide spectrum for a long time while maintaining a stable single-pulse mode-locking state, we tested the long-term stability of the laser, which will be discussed in detail later. Figure 3(d) shows the RF spectrum of the pulse with a fundamental frequency repetition of 755 kHz, the same as in the first-order Raman spectrum output state. The SNR is ∼ 58 dB, indicating stable operation of the ultra-flat broad-spectrum output. The inset in Fig. 3(d) shows no periodic envelope or fluctuations in the 50-MHz span RF spectrum, confirming the laser's stable single-pulse mode-locking performance. In the ultra-flat broad spectrum mode, at a pump power of 0.5 W, the average output power is 2 mW, corresponding to a single pulse energy of 2.65 nJ.

To evaluate the long-term stability of the fiber laser in a broad spectrum output state, tests were conducted at a pump

power of 0.55 W, as shown in Fig. 4.

Figure 4(a) illustrates the spectral evolution over 2 hours at this pump power. The spectral shape remains largely unchanged, with the 6-dB bandwidth stable between 64.45 nm and 65.49 nm and fluctuations in spectral width under 0.05 nm, indicating consistent spectral width and flatness. Figure 4(b) depicts the pulse evolution over 2 hours at the same pump power. The pulse shape, width, and intensity show no significant changes, and the single-pulse mode-locking state remains stable throughout the experiment without transitioning to a multi-pulse state. These results demonstrate that our laser design exhibits excellent long-term stability, making it suitable for practical engineering applications with long-term operational requirements. Moreover, the laser can maintain stable single-pulse mode-locking during the output of a super-flat broad spectrum. Our research solves the problem that lasers find it difficult to maintain stable single-pulse mode-locking in the output of a wide spectrum state. It provides a favorable reference for the experimental design of wide-spectrum single-pulse mode-locking fiber lasers.

Subsequently, the evolution of the laser's output spectrum and pulse was examined as the pump power was increased from 0.5 W to 2.25 W, as depicted in Fig. 5. Figure 5(a) illustrates the spectral evolution: initially, a smooth spectrum was obtained at the pump power of 0.5 W. As the pump power was increased, the spectrum gradually broadened. At the pump power of 1.5 W, a spectral peak began to emerge on the long-wavelength side. With further power increases, this peak widened and heightened, eventually merging with the main broad spectrum peak above 2 W. Ultimately, at 2.25 W pump power, an ultra-wide spectrum with a 20-dB bandwidth approaching 100 nm was formed.

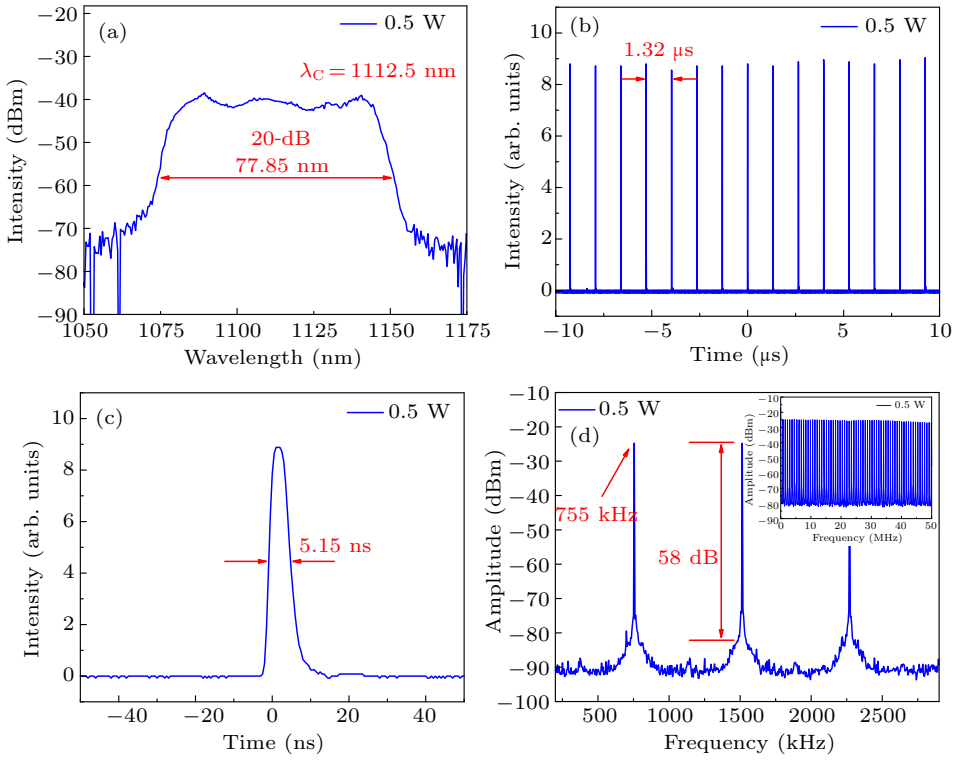


Fig. 3. Output characteristics of ultra-flat wide spectrum: (a) spectrum, (b) pulse sequence, (c) single pulse, (d) RF spectrum with a fundamental frequency of 755 kHz (inset: RF spectrum with a bandwidth of 0 MHz–50 MHz).

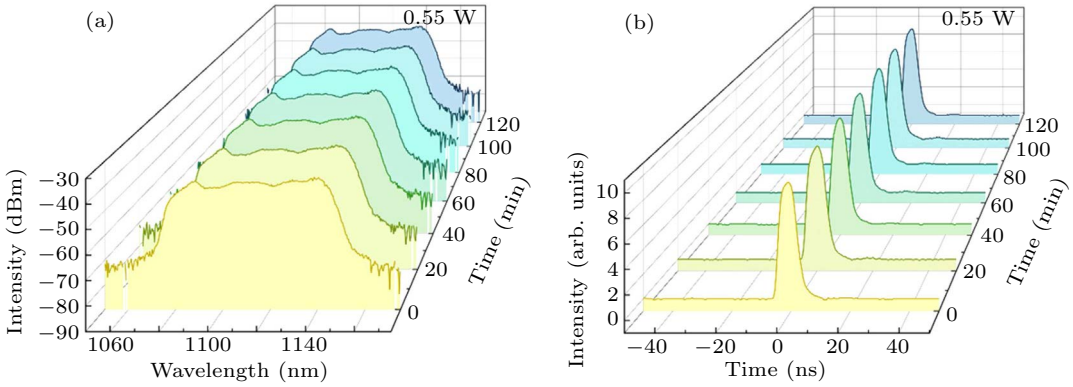


Fig. 4. Long-term operating stability of the laser at 0.55-W pump power: (a) spectrum evolution, (b) pulse evolution.

Figure 5(b) illustrates the pulse evolution with increasing pump power. At the pump power of 0.5 W, a regular single pulse is generated. As power increases, the pulse broadens and their tops start to split, though the bottoms remain connected. At the pump power of 0.75 W, small notches appear on the pulse tops, and beyond 1 W, the pulse becomes distinctly wavy and jittery.

At the pump power of 2.25 W, an ultra-wide spectrum with a 20-dB bandwidth near 100 nm is obtained, as shown in Fig. 6(a). The pulse train and corresponding single pulse in this state are depicted in Figs. 6(b) and 6(c). The pulse interval remains 1.32 μs, consistent with the cavity's round-trip time, and the pulse FWHM is approximately 75.4 ns. Unlike the regular single pulse in the ultra-flat broad spectrum state, the pulse here exhibits irregular wave-like jitter on its tops and has a much larger width. The characteristics of the obtained pulses are very similar to those of dissipative soliton resonance (DSR). Just as the pulse usually has a wider pulse width and peak power clamping effect, more importantly, the pulse is broadened at high pump power rather than split.[32] DSR pulses are a special type of output pulse for mode-locked fiber lasers. Compared with the general solitons generated by fiber lasers, as the gain increases, the peak power of the pulse in the DSR state can remain constant, while the pulse width increases almost linearly, which means that the pulse energy can theoretically increase infinitely.[38] Figure 6(d) shows the RF spectrum of the pulse, maintaining a fundamental repetition frequency of 755 kHz and an SNR of ∼ 56 dB, indicating a stable mode-locked operation. At the pump power of 2.25 W, the average output power is 12 mW, corresponding to a single-pulse energy of 15.89 nJ.

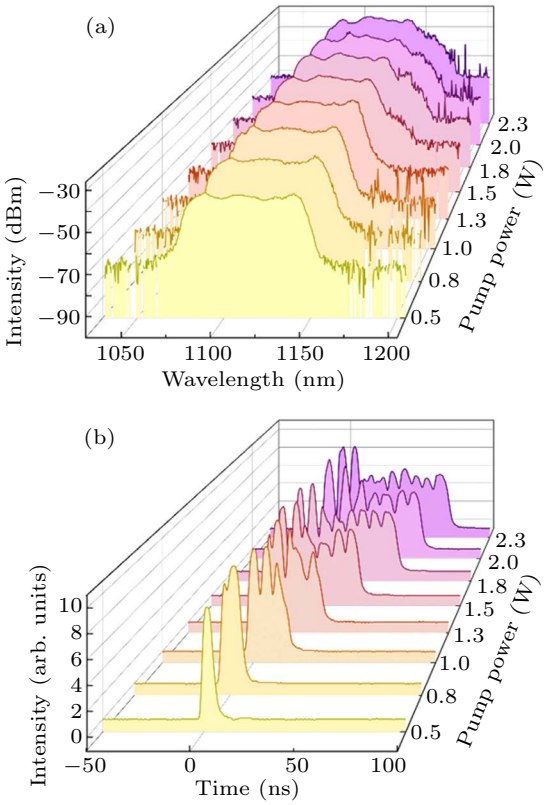


Fig. 5. The evolution of the wide spectrum and its pulse with pump power: (a) spectrum evolution, (b) pulse evolution.

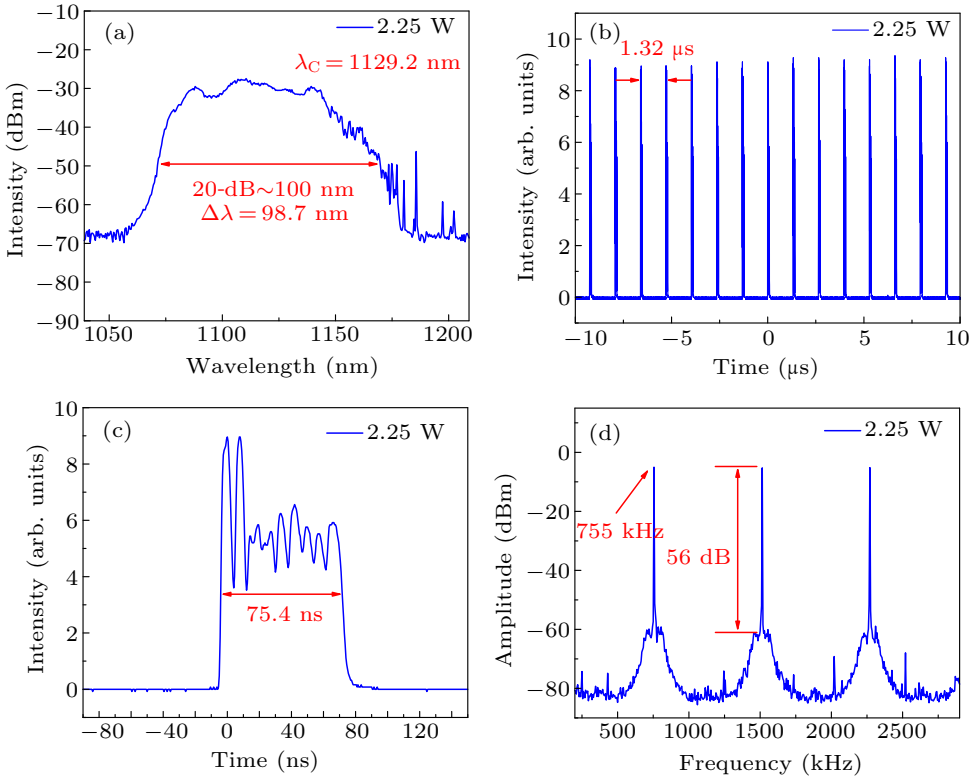


Fig. 6. Output characteristics of nearly a hundred nanometers wide spectrum: (a) spectrum, (b) pulse sequence, (c) single pulse, (d) RF spectrum.

3.2. Pulse bursts

Subsequently, in order to explore the pulse burst phenomenon in the first-order Raman state, PC1 and PC2 are fixed in the first-order Raman single-pulse output state of Subsection 3.1, and the pump power is gradually increased. Then we observe pulse bursts phenomena, with pulse groups reaching up to 9 pulses. As the pump power increases from 0.45 W to 2.25 W, new pulses always appear at the trailing edge of the burst on the time axis, and the pulse number of bursts increases from 1 to 9, as shown in Fig. 7. Prior works on pulse bursts featuring first-order Raman frequency shift demonstrated lower pulse counts: in Refs. [33,34], the authors reported up to 6 pulses, while those in Ref. [36] achieved 8 pulses. In contrast, our work establishes a new record of 9 stable pulses under equivalent conditions. As far as we know, our research achieves the highest pulse count of 9 in a stable mode-locked state with a first-order Raman frequency shift. Moreover, compared to the design in Ref. [36], our laser employs a shorter Raman gain medium.

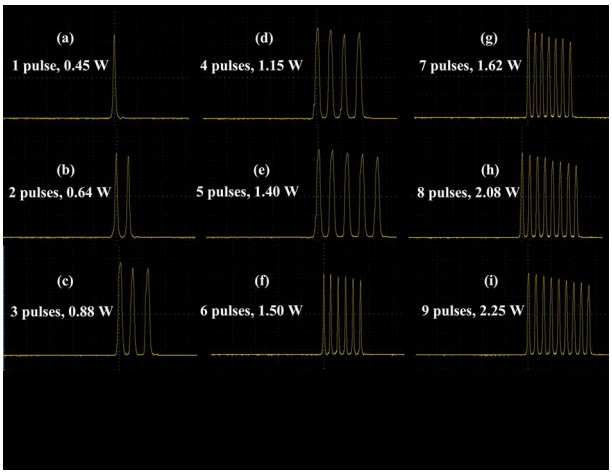


Fig. 7. Pulse burst under the first-order Raman scattering.

As shown in Fig. 7, every pulse in the pulse group maintains the same shape, featuring a steep front edge and a gentler trailing edge. The consistent shape of single pulses within pulse groups indicates that the pulse burst is stable. Moreover, pulse groups with different pulse counts have the same repetition frequency as in the single-pulse state (755 kHz), and each pulse in a group has nearly identical peak power and pulse width. The average output power of the laser for pulse numbers ranging from 1 to 9 is 2 mW, 4 mW, 6 mW, 8 mW, 10 mW, 12 mW, 13 mW, 14 mW, and 16 mW, respectively.

During the pulse burst process, the phenomenon of successive decrease in pulse energy was observed, which can be attributed to the synergistic effect of Raman conversion and the competitive effect of intracavity gain. When the pump power is increased above the threshold, the first generated pulse transfers part of its energy to a longer Stokes wavelength through stimulated Raman scattering during transmission within the fiber cavity. During this process, the energy of the pulse itself is lost due to Raman conversion, and it absorbs energy first in the ytterbium-doped fiber, resulting in gain saturation. Therefore, the subsequent pulses face double limitations when propagating: on the one hand, they are transmitted in the Stokes light field excited by the previous pulses, which is equivalent to propagating in a medium with partially exhausted energy, thereby further losing energy through the SRS effect; on the other hand, due to the limited recovery time of the gain medium, the available gain decreases when the subsequent pulse arrives, forming a negative feedback chain of energy competition. The cumulative effect of this energy transfer is manifested as the monotonically decreasing pulse energy in the pulse train.

Considering the maximum power that the intracavity components (PD-ISO and OC) can withstand, the pump power was not increased beyond 2.25 W. Based on current experimental observations, without the limitation of the maximum power capacity of the components, further increasing the pump power might result in pulse groups with more than 10 pulses. However, it could also disrupt the pulse mechanism once the pump power exceeds a certain threshold.[34,36] According to the pulse-breaking theory based on spectral filtering, Raman scattering-induced spectral broadening might be one of the factors that trigger pulse-breaking.[36] The Raman effect at high pump powers can affect the laser bandwidth and impede the formation of pulse-breaking.

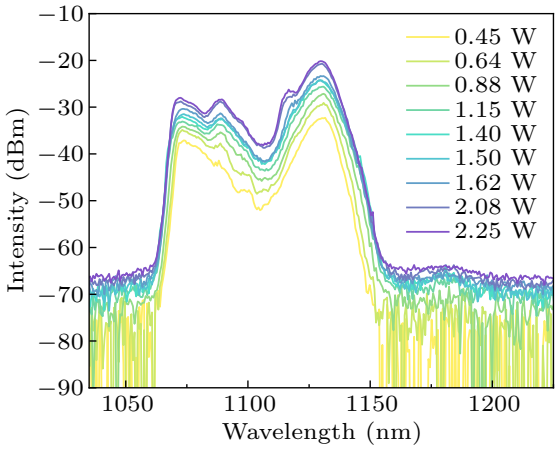


Fig. 8. Spectrum evolution during pulse bursts.

Figure 8 shows the spectrum evolution during pulse-breaking. The spectra in pulse bursts and single-pulse modes are similar but have different intensity levels at various pump powers. The sharp, steep peaks on either side of the spectrum indicate the SPM effects in the cavity.[36] As the pump power increases, the number of pulses in the group and the Raman effect in the cavity both increase. Higher pump powers and more pulses in the group lead to stronger fundamental and first-order Stokes light, broader spectra, and shallower gaps between them, making the spectrum flatter. Particularly, the progressive gap reduction between fundamental and Stokes components suggests the emergence of nonlinear coherence

effects, potentially involving cross-phase modulation mediated by multiple pulse interactions.

It is worth noting that the ultra-flat broad spectrum state (Fig. 3) and the first-order Raman state (Fig. 2) represent two fundamentally distinct mode-locking regimes, achieved by rotating intracavity polarization controllers (PCs). In the ultra-flat state, increasing pump power induces continuous pulse broadening without splitting (Fig. 5), characteristic of dissipative soliton resonance (DSR).[32,38] In contrast, keeping the polarization state of the laser unchanged, the Raman state evolves into pulse bursts under higher pumping (Fig. 7), where pulse energy progressively decreases due to cascaded Raman conversion depleting leading pulses and gain competition.

4. Conclusion

In this study, an ultra-flat broad spectrum with a stable single-pulse mode-locking in a double-clad Yb-doped Raman fiber laser was demonstrated. By adjusting the PCs, we achieved an ultra-flat broad spectrum with a 20-dB bandwidth of 77.85 nm and a 6-dB bandwidth of 67.5 nm, featuring a flatness better than 4 dB. Unlike previous studies, where the pulse output is chaotic and irregular in a broad spectrum state, our fiber laser design ensures a stable single-pulse mode-locking state while outputting an ultra-flat broad spectrum and maintaining that state over a long period. As the pump power increased to 2.25 W, the laser produced an ultra-wide spectrum with a 20-dB bandwidth approaching 100 nm.

In addition, our laser obtained a pulse train of 9 pulses at a pump power of 2.25 W. To our knowledge, this is the largest number of pulses in the pulse bursts phenomenon which involves first-order Raman frequency shift. In conclusion, our research solves the problem that the lasers find it difficult to maintain stable single-pulse mode-locking in a wide spectrum output state. It provides a good reference for the experimental design of wide-spectrum single-pulse mode-locking fiber lasers.

Acknowledgements

Project supported by the National Natural Science Foundation of China (Grant No. 12204132), the Natural Science Foundation of Shandong Province, China (Grant No. ZR2021MF122), Shandong Province Technology-Based SME Innovation Enhancement Project (Grant No. 2024TSGC0715), and the Postgraduate Education Reform Project of Shandong Province, China (Grant No. SDYJSJGC2024107).

References

[1] He X, Lin Q, Guo H, Sun J, Bai J, Hou L and Wang K 2019 *Appl. Phys. Express* **12** 072007
[2] Fermann M E and Hartl I 2009 *Laser Phys. Lett.* **6** 11
[3] Tauser F, Leitenstorfer A and Zinth W 2003 *Opt. Express* **11** 594
[4] Gattass R R and Mazur E 2008 *Nat. Photon.* **2** 219
[5] Wang N, Cai J H, Qi X, Chen S P, Yang L J and Hou J 2018 *Opt. Express* **26** 1689
[6] Hernandez-Garcia J C, Pottiez O and Estudillo-Ayala J M 2012 *Laser Phys.* **22** 221
[7] Lin S S, Hwang S K and Liu J M 2014 *Opt. Express* **22** 4152
[8] Fermann M E and Hartl I 2013 *Nat. Photon.* **7** 868
[9] Chang G and Wei Z 2020 *iScience* **23** 101101
[10] Gao X, Zhao Z, Cong Z, Gao G, Zhang A, Guo H, Yao G and Liu Z 2021 *Opt. Express* **29** 9021
[11] Dong Z, Lin J, Li H, Zhang Y, Gu C, Yao P and Xu L 2020 *Opt. Laser Technol.* **130** 106337
[12] Hu P, Mao J, Zhou X, Feng T, Nie H, Wang R, Zhang B, Li T, He J and Yang K 2023 *Opt. Laser Technol.* **161** 109218
[13] Zheng W, Ruan S, Zhang M, Liu W, Zhang Y and Yang X 2013 *Opt. Laser Technol.* **50** 145
[14] Shang X, Guo L, Gao J, Jiang S, Han X, Guo Q, Chen X, Li D and Zhang H 2019 *Appl. Phys. B* **125** 193
[15] Woodward R and Kelleher E 2015 *Appl. Sci.* **5** 1440
[16] Peng J, Zhu R, Shen T, Liu Y, Ma Y and Gu F 2023 *Photonics* **10** 543
[17] Wang G, Baker-Murray A A and Blau W J 2019 *Laser Photonics Rev.* **13** 1800282
[18] Ming Z and Tianshu W 2024 *J. Appl. Opt.* **45** 834
[19] Ahmad H, Lutfi M A M, Ortaç B, Zaini M K A and Samion M Z 2024 *Optical Fiber Technology* **87** 103861
[20] Hönninger C, Plötner M, Ortaç B, Ackermann R, Kammel R, Limpert J, Nolte S and Tünnermann A 2009 *Proc. SPIE* 7203, Commercial and Biomedical Applications of Ultrafast Lasers IX, 72030W (24 February 2009)
[21] Kumar M, Islam M N, Terry F L, Freeman M J, Chan A, Neelakandan M and Manzur T 2012 *Appl. Opt.* **51** 2794
[22] Mingareev I, Weirauch F, Olowinsky A, Shah L, Kadwani P and Richardson M 2012 *Opt. Laser Technol.* **44** 2095
[23] Seddon A B 2011 *Int. J. Appl. Glass Sci.* **2** 177
[24] Hui Z, Zhang X, Xu W, Li N and Li X 2023 *Optics & Laser Technology* **157** 108712
[25] Ahmad H, Ahmed M H M, Yusoff N, Ramli R and Samion M Z 2020 *Optics & Laser Technology* **130** 106350
[26] Song R, Hou J, Chen S, Yang W and Lu Q 2012 *Opt. Lett.* **37** 1529
[27] Gao J, Ge T and Wang Z 2014 *Opt. Eng.* **53** 86109
[28] Wang H, Han H, Shao X, Zhang Z, Zhu J and Wei Z 2022 *Appl. Phys. B* **128** 25
[29] Agrawal G P 2000 *Nonlinear fiber optics/Nonlinear Science at the Dawn of the 21st Century* (Berlin, Heidelberg: Springer Berlin Heidelberg), 2000 pp. 195–211
[30] Alcántara-Bautista U, Durán-Sánchez M, Addiel Espinosa-De-La-Cruz E, Armas-Rivera I, Bello-Jiménez M and Ibarra-Escamilla B 2024 *Optics & Laser Technology* **168** 110016
[31] Carrillo-Delgado C M, Hernandez-Garcia J C, Estudillo-Ayala J M, Pottiez O, Lauterio-Cruz J P, Filoteo-Razo J D, Jauregui-Vazquez D, Sierra-Hernandez J M and Rojas-Laguna R 2020 *Laser Phys. Lett.* **17** 065106
[32] Zhang B, Chen X, Zhang X, Liu Z, Li M, Liu J, Xu L, Hu Q and Li P 2022 *Infrared Physics & Technology* **120** 103990
[33] Manriquez-Cobian N, Hernandez-Garcia J C, Estudillo-Ayala J M, Pottiez O, Filoteo-Razo J D and Rojas-Laguna R 2024 *Optics & Laser Technology* **172** 110530
[34] Dong T, Lin J, Gu C, Yao P and Xu L 2021 *Opt. Commun.* **484** 126679
[35] Li X, Zhang S, Hao Y and Yang Z 2014 *Opt. Express, OE* **22** 6699
[36] Liu J, Li P, Li M, Chen X, Zhang B, Xu L, Hu Q and Gao L 2022 *Optik* **251** 168490
[37] Yu H, Wang X, Zhou P, Xu X and Chen J 2014 *Appl. Phys. B* **117** 305
[38] Liu C, Cao Y, Tang X, Tang M and Zhao L 2022 *Chin. J. Lasers* **49** 2100002